Available online at www.sciencedirect.com
ScienceDirect
C. R. Physique 8 (2007) 165–179
COMPTES RENDUS PHYSIQUE
http://france.elsevier.com/direct/COMREN/

Recent advances in crystal optics/Avancées récentes en optique cristalline

Nonlinear polarimetry of molecular crystals down to the nanoscale

Sophie Brasselet *, Joseph Zyss

Laboratoire de photonique quantique et moléculaire, institut d'Alembert, École normale supérieure de Cachan, 61, avenue du président Wilson, 94235 Cachan, France

Available online 10 October 2006

Invited Paper

Abstract

Molecular nonlinear optics is currently experiencing a fruitful revival as a result of the unprecedented possibility to experimentally access the nanoscale through adequate nanophotonics instrumentation and modelling. It is the purpose of this article to survey and discuss some ongoing developments in this domain within our laboratory, with special emphasis on polarization dependent tensorial properties read-out at submicron scale, to be exploited towards a better understanding of nanostructured architectures, ordering as well as dynamical crystallization properties of a variety of samples, down to the spatial resolution of two-photon nonlinear confocal microscopy. The advantages of combining coherent (e.g. second harmonic generation) and incoherent (e.g. two photon induced fluorescence) phenomena, moreover with polarization resolution, will be shown to open-up a new and unique pathway onto the orientation as well as crystalline quality of different types of nanocrystals (from one component molecular to mixed guest–host binary crystals). The oriented gas model, expressed in its most general invariant form by way of irreducible multipolar decomposition permits to identify generic types of nonlinear polarization patterns which potentially provide both qualitative and quantitative insight onto the structural properties of a broad variety of molecular as well as inorganic nanomaterials. ***To cite this article: S. Brasselet, J. Zyss, C. R. Physique 8 (2007).***

Résumé

Polarimétrie non-linéaire sur des cristaux moléculaires jusqu'à l'échelle nanométrique. L'optique non-linéaire en milieux moléculaires est actuellement en phase de renouvellement au débouché de la possibilité nouvelle d'accéder aux échelles nanométriques grâce à une instrumentation nano-photonique de pointe et aux modèles associés. Nous nous proposons dans cet article de passer en revue et de discuter des développements en cours dans ce domaine dans notre laboratoire, en mettant particulièrement en exergue les propriétés tensorielles de dépendance en polarisations résolues à une échelle submicronique, aux fins d'une meilleure compréhension des architectures de nanostructures, de l'ordre et des propriétés dynamiques de cristallisation jusqu'à la résolution de la microscopie confocale à deux photons. L'intérêt de combiner les effets non-linéaires cohérents (i.e. génération de second harmonique) et incohérents (i.e. fluorescence à deux photons) tous deux résolus en polarisation apparaît dans la possibilité de déterminer l'orientation et la qualité cristalline de nano-cristaux (depuis des cristaux mono-moléculaires jusqu'à des cristaux binaires de type hôte-matrice). Le modèle de gaz orienté, interprété de la façon la plus générale en symétries multipolaires grâce au formalisme des tenseurs irréductibles, permet d'identifier des formes génériques de réponses angulaires en polarisation dont l'allure renseigne qualitativement et quantitativement sur les propriétés structurelles d'une large variété de nanomatériaux organiques et inorganiques. ***Pour citer cet article : S. Brasselet, J. Zyss, C. R. Physique 8 (2007).***

* Corresponding author.
E-mail address: sophie.brasselet@lpqm.ens-cachan.fr (S. Brasselet).

1631-0705/$ – see front matter
doi:10.1016/j.crhy.2006.07.015

Keywords: Nanoparticle; Nonlinear optics

Mots-clés : Nanoparticule ; Optique non-linéaire

1. Introduction

Recent demonstrations of targeted fabrication of molecular nanoparticles have opened new perspectives in nanosciences, covering a wide range of fundamental investigations and applications in physics, chemistry and biology. The research on fabrication of organic-based crystalline nanoparticles has generated a large number of technical developments, including evaporation of organic molecules [1], re-precipitation [2] microwave irradiation [3] laser ablation [4] crystallization in a sol–gel matrix [5] as well as co-crystallization with inorganic compounds [6].

Research on molecular nanocrystals is currently concentrating on fluorescence applications, along the major goal of obtaining reduced-size efficient emitters. Such nanocrystals, which exhibit intense emission, low photobleaching rates and potentialities towards nanosensing of ions and charges, represent an interesting and possibly advantageous alternative to current single molecule and semiconductor nanoparticles. Assembling organic molecules within nanometric sizes also provides a new scale of investigation of molecular interactions, such as modifications of linear optical effects due to strong intermolecular interactions. Moreover, confinement down to nanometric scales allows the enhancement of fluorescence emission, first because of the large number of emitters to be packed in a small-size object, second because of possible excitonic effects [7]. Such nanoparticles offer a large range of potential applications from nanoscale photonics to nanoprobes with original optical properties [8].

Engineering non-centrosymmetric molecular nanoparticles has been achieved by various techniques, such as fast crystallization of nonlinear molecules during sol–gel thin films deposition [5], or templating hybrid organic–inorganic systems into polar order for active molecules [9]. Nevertheless, the design of such nano-objects for coherent nonlinear optics applications is still in its infancy mainly because characterization methods for non-centrosymmetric ordering are limited at such scales. Quantifying the nonlinear response of such objects has been mainly based so far on Hyper Rayleigh Scattering (HRS) measurements in solution, which provides a non-coherent averaged response over an ensemble of nanoparticles [9,10]. The main limitation of HRS is that important structural information such as size homogeneity, in situ disorder and possible aggregation cannot be directly evidenced. Such information can only be unravelled by the exploration of individual objects, which requires nonlinear microscopy imaging techniques with high spatial resolution. In that respect, second harmonic generation (SHG) microscopy has received a considerable interest for its ability to probe non-centrosymmetry at the nanometric scale in molecular media such as monolayers [11,12], inorganic nanostructures [13], organic or inorganic nanoparticles [14,15], as well as biological media [16]. Inverted nonlinear microscopy is particularly suitable for such investigations since the reduced size of the focus spot allows one to unscramble the SHG signal from propagation conditions such as imposed by phase matching and other cumulative phenomena along the propagation pathway.

In this article, we describe a generalized application of nonlinear microscopy approach combining two photon imaging, both coherent and non-coherent, with polarimetry analysis, either from individual particles or assemblies of molecules. Such a technique provides deeper local information on molecular orientations and distribution order parameters [12,17]. In the context of nonlinear crystals of various sizes, we describe the specific properties and information gained by the measurement of two-photon induced nonlinear processes. We show that the combination of SHG with two-photon induced fluorescence (TPF) detection is able to probe orientation of nano-objects as well as orientational disorder, providing a diagnostic of monocrystallinity in organic nanostructures [14]. We analyse such properties in the context of crystalline objects of various multipolar symmetries. In particular, in order to retrieve information on the three dimension (3D) orientation of one-dimensional objects, we show that 2D polarization analysis is no longer applicable and that additional techniques such as radiation pattern imaging are required. Nonlinear microscopy is thus a versatile tool capable of providing a framework for a broad range of studies such as targeting particles for nonlinear nanosources, nanosensors, and nanofrequency mixers.

2. Nonlinear two-photon microscopy processes in complex media

Although one-dimensional molecules and arrangements exhibit a very simple geometry, optimized along one direction of molecular-field interactions, it has been shown during the last decades that multipolar geometries, at the

molecular scale as well as at the macroscopic scale, exhibit significant advantages [18,19]. The major consequence of a multipolar arrangement is the complexity and flexibility of polarization responses obtained in nonlinear processes, the more significant example being the recent demonstration of polarization independence responses of second harmonic generation in octupolar crystals [20,21].

Nonlinear susceptibilities in multipolar system exhibit, however, a high number of Cartesian coefficients, coupling to external field either at the stage of molecular orientation [19] or for structural probing by linear or nonlinear optical processes. The introduction of 'reading tensorial fields' [22] and the decomposition of high order tensors on invariant bases [18] has allowed one to considerably simplify the molecular-field interactions in multipolar complex systems [19].

In the present work, only two-photon excitation induced effects are considered. Two-photon excitation processes are known to potentially generate both coherent processes such as SHG, and incoherent ones such as TPF. In non-centrosymmetric molecules, approaching resonant excitation levels via two-photon excitation at frequency ω leads to generation of one photon coherent emission at 2ω (SHG) as well as relaxation to the ground state by means of a fluorescent (one-photon) emission (TPF). The origins of both processes are distinct, and pertain to specific light-matter interactions involving different molecular susceptibility tensors.

In the case of SHG, the nonlinear polarization can be written $p^{2\omega} = \beta \cdot F^{\mathrm{SHG}}$, with β the second order molecular nonlinear susceptibility tensor, and $F^{\mathrm{SHG}} = e \otimes E^{\omega} \otimes E^{\omega}$ the reading field for SHG [20,21], generated by an incident fundamental field E^{ω} and read-out by an analysis direction e [22]. In the case of TPF analyzed along e, the signal is proportional to the product of the excitation and emission probabilities $|\mu_{\mathrm{abs}} \cdot E^{\omega}|^4 \cdot |\mu_{\mathrm{em}} \cdot e|^2 = (\alpha \otimes \gamma) \cdot F^{\mathrm{TPF}}$, with $F^{\mathrm{TPF}} = e \otimes e \otimes E^{\omega} \otimes E^{\omega} \otimes E^{\omega *} \otimes E^{\omega *}$ the associated reading field. The one-photon emission tensor α and the two-photon excitation tensor γ are in practice imaginary parts of the corresponding first and third order susceptibilities. The resulting intensities in the most general case of a statistical distribution $f(\Omega)$ of the molecular orientations, accounting for the coherent nature of SHG and for the incoherent nature of TPF are [17]:

$$I_e^{\mathrm{SHG}} = N^2 \int \left|\beta(\Omega) \cdot F^{\mathrm{SHG}}\right|^2 f(\Omega)\,\mathrm{d}\Omega \quad \text{and} \quad I_e^{\mathrm{TPF}} = N \int \left[(\alpha \otimes \gamma)(\Omega) \cdot F^{\mathrm{TPF}}\right] f(\Omega)\,\mathrm{d}\Omega \tag{1}$$

with N the number of molecules illuminated by the fundamental field, and $\beta(\Omega) = R_{\Omega}(\beta)$ the expression of the molecular tensor in the macroscopic frame. The N dependence of TPF confirms its incoherent nature, whereas the coherent SHG signals exhibit a N^2 dependence. The local field coefficients are not included here for the sake of simplicity, as in the following analyses. The efficiency evaluations however account for such factors.

Eq. (1) also shows the determinant symmetry properties of the SHG and TPF reading processes. Since the molecular tensors α, β and γ are respectively of 1st, 2nd and 3rd order, the investigation of molecular angular order parameters using optical processes will therefore allow for filtering and hence discrimination of odd orders of $f(\Omega)$ (in the case of a SHG reading), from even orders (in the case of a TPF reading). Such complementarity has been advantageously exploited to provide complete information on complex molecular distributions [17,23]. In order to unify such symmetry rules of molecular-field interactions, a more general picture can be derived from decomposition of tensorial molecules and fields on normalized spherical harmonics $C_m^J(\theta, \phi)$ [24,25]. The J orders correspond to the symmetry orders of molecular susceptibility which decompose along the coefficients β_m^J, α_m^J and γ_m^J. Such coefficients are invariant by rotation, which is of essential use for molecular-fields interactions studies in the macroscopic frame. Far from resonances, the β_m^J only involve the odd $J = 1$ (dipolar) and $J = 3$ (octupolar) orders [18], whereas α_m^J contains $J = 0, 2$ terms and γ_m^J contains $J = 0, 2, 4$ terms. The filtered terms of the molecular angular distribution function, which are expressed in the decomposition $f(\Omega) = \sum_{m',m,J} f_{m'm}^J D_{m'm}^J(\Omega)$ on the Wigner matrices, are therefore and $f_{m'm}^{J=1,3}$ using SHG, probing non-centrosymmetry, and $f_{m'm}^{J=0,2,4,6}$ using TPF, probing centrosymmetric anisotropies.

In the case of crystals, the molecular distribution is set by the unit cell symmetry and its orientation Ω_0 in the macroscopic frame (X, Y, Z). Therefore

$$I_e^{\mathrm{SHG}}(\Omega_0) = N^2 \left|\beta(\Omega_0) \cdot F^{\mathrm{SHG}}\right|^2 \quad \text{and} \quad I_e^{\mathrm{TPF}}(\Omega_0) = N(\alpha \otimes \gamma)(\Omega_0) \cdot F^{\mathrm{TPF}} \tag{2}$$

where N stands here for the number of unit cells number illuminated by the fundamental field. The unit cell tensors α, β and γ can be expressed in the unit cell frame work using the $(i, j, k) = (1, 2, 3)$ indexes as well as in the macroscopic framework, using the $(I, J, K) = (X, Y, Z)$ indexes. The relation between the two frame representations can be expressed following both Cartesian and irreducible formalisms [26]. In the case of the β tensor

$$\beta(\Omega_0)_{IJK} = R_{\Omega_0}(\beta)_{IJK} = \sum_{i,j,k} \beta_{ijk}(i\cdot I)(j\cdot J)(k\cdot K)(\Omega_0)$$
$$\beta(\Omega_0)^J_m = R_{\Omega_0}(\beta)^J_m = \sum_{m'} \beta^J_{m'} D^J_{m'm}(\Omega_0) \tag{3}$$

Note that unit cell coefficients can be readily obtained from knowledge of the molecule nonlinear coefficients $\beta^{\text{molecule}}_{i_m j_m k_m}$ (where (i_m, j_m, k_m) denotes the molecular axes) and their orientation in the unit cell. Therefore Eq. (3) can also be written: $\beta(\Omega_0)_{IJK} = \sum_{m=1\ldots M} \sum_{i_m,j_m,k_m} \beta^{\text{molecule}}_{i_m j_m k_m}(i_m\cdot I)(j_m\cdot J)(k_m\cdot K)(\Omega_0)$ where M is the number of molecules per unit cell [27].

The invariant expressions of the SHG and TPF macroscopic responses can finally be written in a crystal using the most generally used oriented gas model [27] in an invariant picture as

$$I_e^{\text{SHG}}(\Omega_0) = N^2 \left| \sum_{m,J=1,3} \beta(\Omega_0)^J_m \left(F^{\text{SHG}}\right)^{J^*}_m \right|^2 \quad \text{and} \quad I_e^{\text{TPF}}(\Omega_0) = N \sum_{m,J=0,2,4} (\alpha\otimes\gamma)(\Omega_0)^J_m \left(F^{\text{TPF}}\right)^{J^*}_m \tag{4}$$

It is therefore clearly visible, from Eq. (4), that only the corresponding reading tensorial orders are able to read out the corresponding molecular order properties, and in particular retrieve information on either the unit cell symmetry (J orders), or on the unit cell orientation (Ω_0 parameter). Such selection rules are hidden in a purely Cartesian formalism [22]. In the following section, the Cartesian expression will be mostly used in order to demonstrate the benefit of polarimetric analyses.

3. Retrieving crystalline information in nano-objects using nonlinear two-photon microscopy

The coherent nature of SHG provides distinctive features to be outlined. In particular, the investigation of nonlinear responses from crystalline nanoscale objects (or from a macroscopic objects investigated within a sub-wavelength scale excitation volume) requires a new approach which does not involve propagation analysis, since the signals are integrated over distances below the coherence length. Considering an ensemble of N nonlinear emitters characterized with their positions $\vec{r}_n$ and orientation angles Ω_n within a nanoscale volume, the nonlinear SHG signal occurs from the coherent build-up from the nonlinear induced dipoles $\vec{p}^{2\omega}(\vec{r}_n, \Omega_n) = \beta(\Omega_n)$: $\vec{E}^{\omega}(\vec{r}_n)\vec{E}^{\omega}(\vec{r}_n)$, where $\vec{E}^{\omega}$ is the incident fundamental field at the ω frequency, $\beta(\Omega_n)$ the hyperpolarizability tensor for a molecule oriented at an angle Ω_n in the macroscopic frame. The nonlinear intensity can then be written, after squaring the above expression, as

$$I^{\text{SHG}} \propto \sum_{n,n'} \mathrm{e}^{\mathrm{i}\Delta\vec{k}\cdot(\vec{r}_n - \vec{r}_{n'})} \vec{p}^{2\omega}_{\perp}(\vec{r}_n, \Omega_n)\vec{p}^{2\omega}_{\perp}(\vec{r}_{n'}, \Omega_{n'})^* \tag{5}$$

where $\perp$ indicates the projection in the transverse polarization plane, $\Delta\vec{k} = 2\vec{k}^{\omega} - \vec{k}^{2\omega}$ is the wavevectors mismatch between the incident ω and harmonic 2ω wavelengths, indicative of constructive or destructive interference effects depending on the distance between emitters and their relative orientation. In the case of a collection of dipoles located within a volume smaller than the SHG coherence length, then $\Delta\vec{k}\cdot(\vec{r}_n - \vec{r}_{n'}) \ll 1$ and therefore the phase factor can be ignored, leading to

$$I^{\text{SHG}}_I \propto \sum_{IJKMN} \sum_{n,n'=1}^{N} \beta_{IJK}(\Omega_n)\beta^*_{IMN}(\Omega_{n'}) E^{\omega}_J E^{\omega}_K E^{\omega^*}_M E^{\omega^*}_N \tag{6}$$

where $(I, J, K, M) = (X, Y, Z)$ refer to coordinates in the macroscopic framework.

Particular cases leading to a reduction of Eq. (6) can be singled out:

– If the molecules are assembled in a crystalline unit cell of orientation Ω_0 in the macroscopic frame, then the signal analyzed along the I polarization direction can be derived from Eq. (2) and expressed as

$$I^{\text{SHG}}_I(\Omega_0) \propto N^2 \left| \sum_{IJK} \beta_{IJK}(\Omega_0) E^{\omega}_J E^{\omega}_K \right|^2 \tag{7}$$

with N the number of unit cells in the focal volume.

– In the case where all the molecules exhibit random orientations, the $n \neq n'$ contributions of Eq. (5) vanishes and only a hyper-Rayleigh contribution remains:

$$I_I^{\mathrm{HRS}} \propto N \sum_n \left|\beta_{IJK}(\Omega_n) E_J^{\omega} E_K^{\omega}\right|^2 \tag{8}$$

The linear dependence in N of this signal is a signature of an incoherent response.

Note that Eqs. (7) and (8) do not account for proportionality factors (such as collection efficiency or integration over the objective aperture). Such parameters are however accounted for in the analysis of experimental polarization responses [17]. In addition, local fields are not indicated and can be considered as included in the β tensors, since their experimental evaluation is not accessible in nano-objects.

In the case of two-photon fluorescence (TPF), the emission of such a similar ensemble is representative of the incoherent emission following two-photon excitation. Assuming for simplicity that the excitation and emission dipoles of the molecule are along identical directions, Eq. (2) can be expressed as:

$$I_I^{\mathrm{TPF}}(\Omega_0) = N\alpha_{II}(\Omega_0) \sum_{JKLM} \gamma_{JKLM}(\Omega_0) E_J^{\omega} E_K^{\omega} E_L^{\omega^*} E_M^{\omega^*} \tag{9}$$

SHG and TPF may co-exist in certain conjugated asymmetric molecular systems, provided that the excitation is close to resonance, in order to generate fluorescence. Corresponding cross-sections of such processes can be inferred using the quantum expression of the involved susceptibilities. Typically in the case of a resonant excitation, $\sigma^{\mathrm{TPF}} = 10^{-50}$ cm^4 s ph^{-1} and $\sigma^{\mathrm{SHG}} = 10^{-53}$cm^4 s ph^{-1} for a functionalized conjugated one-dimensional molecule [28]. Although the TPF cross-section appears to be larger than for SHG, a non-centrosymmetric alignment of molecular dipoles is able to enhance SHG responses, since the coherent build-up of the SHG signal growth with the square of the number of molecules. The orders of magnitude of the respective signals for an incident intensity of $I^{\omega} = 3 \times 10^{24}$ photons^{-1} cm^{-2} (which is typically used in microscopy), are given in Fig. 1. In such conditions, the TPF and SHG signals are of similar magnitudes above a few thousands of molecules in the focal spot, which represent crystals of typical sizes of five to ten nanometers. Using usual detection noise in photon counting detectors, the incoherent Rayleigh signal can be detectable above a number of molecules of about $N \sim 10^6$ [29].

In this work, we use a polarimetry analysis of the nonlinear responses combining both SHG and TPF processes. In practical terms, the incident polarization is being rotated in the (X, Y) sample plane with a variable angle $\Phi = (\vec{X}, \vec{E}^{\omega})$. Such variation induces an angular dependence of the excitation field tensor $E_J^{\omega} E_K^{\omega} E_L^{\omega^*} E_M^{\omega^*}(\Phi)$ which allow us to infer a wealth of information:

– Provided that the crystalline unit cell symmetry is known, the orientation of a nanocrystal can be retrieved from such polarization responses. This is particularly interesting for efficiency estimation on nonlinear nanoparticles, which depends critically on the nonlinear dipoles orientation in the macroscopic frame. However, in the general case, the polarization response at a specific incidence angle is generally not sufficient to retrieve a complete orientation information, since such study reduces the 3D space to its in-plane projection. Along the same lines, bulk crystals investigations require angular incident angle and polarization variations to retrieve nonlinear efficiency

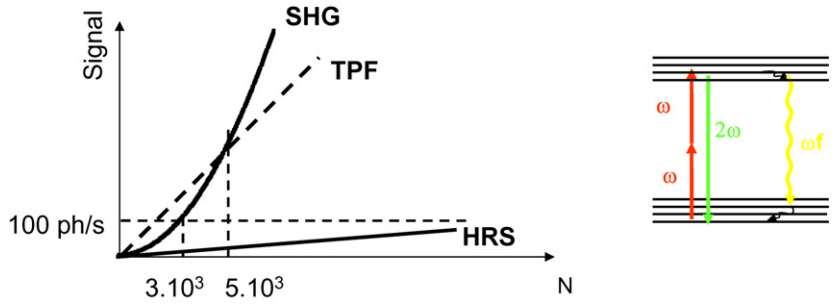

Fig. 1. Order of magnitude of nonlinear two-photon excitation signals in the case of a perfectly aligned ensemble of nonlinear molecules (SHG, TPF) and an amorphous ensemble of such molecules (HRS). The corresponding parameters and equations are given in the text. The horizontal dashed line corresponds to usual noise limits in photon detection in nonlinear microscopy.

information. However, many multipolar symmetries can be reduced to their projection, for which the polarimetric measurement of nonlinear responses at normal incidence is sufficient [29]. Such is the case for the particularly important C_{2v} and octupolar D_{3h} symmetries, as described below.

– Exploration of the TPF 2D polarization responses provides direct and thorough access to the crystalline nature and quality of nano-objects. Indeed in Eq. (9) a separation is possible between the polarization excitation variation dependence denoted $\mathrm{Pol}(\Omega_0, \Phi) = \sum_{JKLM} \gamma_{JKLM}(\Omega_0) E_J^{\omega} E_K^{\omega} E_L^{\omega^*} E_M^{\omega^*}(\Phi)$, and the emission properties, with: $I_I^{\mathrm{TPF}}(\Omega_0, \Phi) = N\alpha_{II}(\Omega_0)\,\mathrm{Pol}(\Omega_0, \Phi)$. Therefore, whatever the orientation of the nanocrystal, the polarization response of TPF exhibits the same shape for any analysis direction I, with an amplitude proportional to the projection $\alpha_{II}(\Omega_0)$. This property provides a direct way of diagnose the monocrystalline quality of a crystal, whatever it scale.

3.1. Nonlinear microscopy

Polarimetry detection in nonlinear microscopy, represented schematically in Fig. 2(a), has been described thoroughly in previous papers [17]. The source is a Ti:Sa laser (150 fs, 86 MHz repetition rate) with a typical average intensity varying between 8×10^4 W cm^{-2} and 8×10^5 W cm^{-2} at an incident wavelength of $\lambda = 780$–1000 nm. An achromatic half-wave plate is placed at the entrance of the microscope in order to continuously vary the polarization direction of the incident light towards polarimetry studies. The laser beam is focused on the sample through a high numerical aperture oil immersion objective ($\times 100$, NA $= 1.4$). The TPF and SHG emissions are collected through the same objective. The emission beam is then divided by a polarizing beam-splitter and orthogonally polarized signals are recorded by two avalanche photodiodes operating in the photon counting regime. The TPF or SHG signal is selected by adequate interference filters chosen according to the emission spectrum, which can be recorded by focusing the signal beam at the entrance fiber of a spectrograph coupled to a highly sensitive CCD camera. The sample is mounted on a piezoelectric scanning system which is translated in its plane with a scan step of 100 nm. The optical resolution of the system is 300–350 nm as estimated from images from calibrated fluorescent nanospheres. The polarization response of the optical signals is recorded and analyzed following a careful calibration of the set-up, which quantifies the dephasing and elliptization introduced by the dichroic mirror and the high numerical aperture of the objective [17,29]. The magnitude measurement of the nonlinear efficiency of the crystals is performed by comparing their nonlinear SHG polarization responses to that from a known $KTiOPO_4$ crystal [30].

Another possible geometry of nonlinear microscopy is based on nonlinear parallel imaging, for which the incident beam convergence is adapted in order to obtain an excitation area of the order of 10–20 μm. Such a scheme, represented in Fig. 2(b), allows us to record images in a dynamic way as described below.

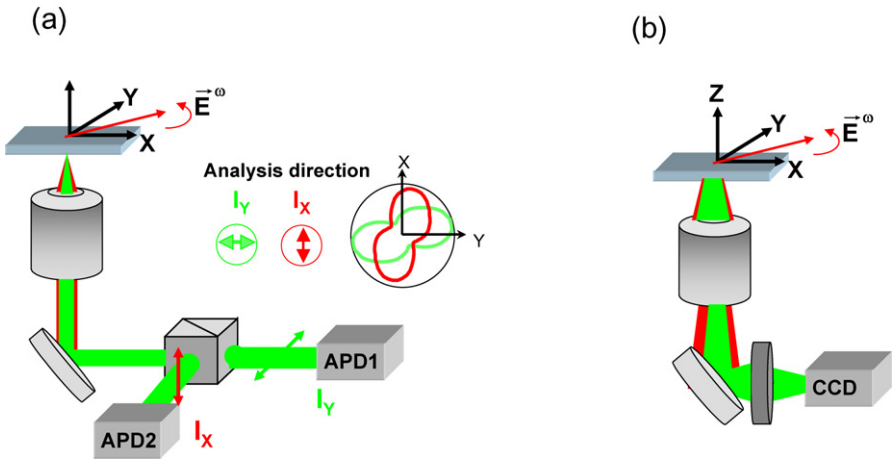

Fig. 2. Nonlinear microscopy set-ups: (a) confocal imaging polarimetry scheme, (b) parallel imaging scheme.

3.2. One-dimensional crystals investigations

Among the recent progress reported in nonlinear molecular engineering for efficient crystals, interesting structures have been engineered by taking advantage of co-crystallization processes involving bulky counter-ions [31,32], hydrogen-bonding partner molecules, or structure-directing templates [6]. Inclusion compounds based on the polycyclic hydrocarbon perhydrotriphenylene (PHTP) system have been intensively investigated [33,34]. Such a host structure forms a pseudo-hexagonal matrix with parallel channels suitable for the inclusion of polar donor–acceptor nonlinear chromophores, with a non-centrosymmetric ordering locally induced by guest–guest head to tail interactions occurring during the crystal growth [35]. Scanning pyroelectric microscopy, as well as phase-sensitive SHG microscopy measurements, which reflect the polarity of the molecular alignment, have provided micrometer-resolution maps of such PHTP-based crystals [35,36]. A double cone structure centered at the nucleation point of the channels has been identified, each side of the cone corresponding to molecules pointing non-centrosymmetric wise towards opposite directions.

Inclusion compound crystals are grown from solution and exhibit micrometric to millimetric-size needle shapes that are suitable for the inverted microscope geometry. Such crystals can be fabricated by slow evaporation under the microscope, and a dynamic growth of SHG during crystallization could be observed using the parallel imaging scheme of Fig. 2(b) (Fig. 3). The local polarization response from such structures can be readily interpreted since the grown crystals are expected to contain parallel molecules lying in the sample plane. In the case of one-dimensional molecules in a one-dimensional geometry arrangement, only α_{33}, β_{333} and γ_{3333} coefficients intervene in Eqs. (8), (9), with '3' indicating the molecular dipoles direction. The polarization response is characteristic of a perfect one-dimensional order, as described below (Fig. 3). Only a few defects were visible in such crystals [37].

The evaluation of the efficiency of PHTP-based crystals, by comparison with a reference $KTiOPO_4$ crystal investigated in the same conditions, has allowed us to estimate the proportion of active molecules contributing to the non-centrosymmetric order. This parameter can be quantified as the net polarity $\Delta N = (N^+ - N^-)$ between the densities of molecules N^+ and N^- pointing in opposite directions [34]. The measured efficiency is then deduced from

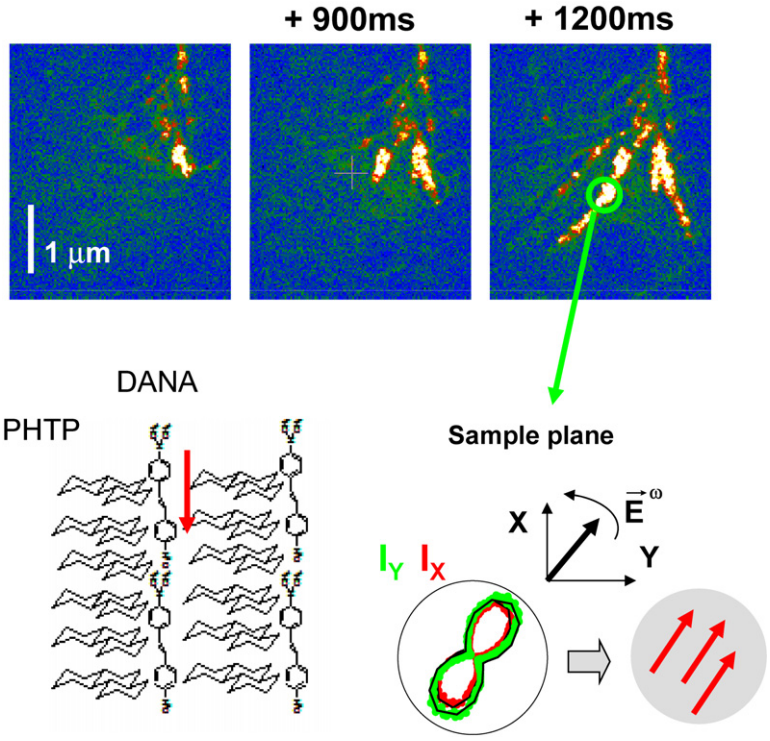

Fig. 3. Dynamic SHG image of a crystal growth of PHTP-DANA inclusion compounds and local polarization response, showing perfect one-dimensional order. A drop of PHTP and the guest compound diluted in 2-butanone was slowly evaporated on the substrate.

$I^{\mathrm{SHG}} = (N^+ - N^-)^2 |\vec{p}^{\mathrm{SHG}}|^2 = (kN)^2 |\vec{p}^{\mathrm{SHG}}|^2$ with $k = \Delta N/N$ the proportion of molecules contributing to the non-centrosymmetric order, N the total density of molecules and $|\vec{p}^{\mathrm{SHG}}|^2$ the nonlinear intensity from a single molecule. Efficiencies up to $d_{33}(0) = 330\ \mathrm{pm\,V^{-1}}$ have been reached in PHTP inclusion crystals containing the DANA molecule 4-dimethylamino-4′-nitroazobenzene, similar to Disperse Red One (Fig. 3) [37]. Knowing molecular efficiencies and estimating local fields magnitudes in the measured crystals, this leads to typical net polarities of $k = 80\%$ in such systems, which is consistent with theoretical analyses [34].

3.3. Octupolar crystals

Among the advantages of octupolar structures is the availability of a broader range of nonlinear tensorial β_{ijk} coefficients (with i, j, k being the molecular frame indexes) compared to the 1D scheme. Such crystalline symmetry may lead to an optimum nonlinear efficiency together with a polarization-independent second harmonic response with respect to the incident light [20,21]. Optimization at the molecular level has shown great progress as exemplified by well established structure-property relationship for two-dimensional octupoles and the development of highly efficient molecules [38–40]. The structure of 1,3,5-tricyano-2,4,6-tris(p-diethylaminostyryl)benzene (TTB) crystal based on octupolar molecules has been elucidated experimentally by the combined polarization analysis of two-photon fluorescence (TPF) and second harmonic generation (SHG) emissions, using a two-photon excitation microscope [21]. The high SHG efficiency resulting from the optimal crystalline packing of the molecules in an octupolar symmetry, originating from intermolecular π–π lamellar stacking interactions, results in a very large crystal nonlinear efficiency $d_{11}(0) = 96\ \mathrm{pm\,V^{-1}}$, together with the benefit of nonlinear in-plane isotropy [20,21].

In the case of a pure D_{3h} octupolar geometry in the $(1, 2)$ crystalline plane, only a limited number of susceptibilities coefficients are non-vanishing, namely: $\alpha_{11} = \alpha_{22} = 1/\sqrt{2}\|\alpha\|$ ($\|\alpha\| = \sum_{ij} \alpha_{ij}^2$ is the tensorial norm), $\gamma_{1111} = \gamma_{2222} = 0.612\|\gamma\|$, $\gamma_{1122} = \gamma_{2211} = \gamma_{1221} = \gamma_{2112} = \gamma_{2121} = \gamma_{1212} = \gamma_{1111}/3 = 0.204\|\gamma\|$, and $\beta_{111} = -\beta_{122} = -\beta_{212} = -\beta_{221} = 0.5\|\beta\|$. The polarization analysis is therefore simplified and exhibits remarkable features that are specific of this geometry. In particular, contrary to a pure 1D symmetry, the SHG polarization plots show very strong sensitivity to the tilt angle of the unit cell with respect to the sample plane. The shape of a SHG polarization response as a 2D polar plot is therefore a sensitive signature of the tilt angle of the unit-cell, whereas in the one-dimensional case, the polar plot exhibits the same shape whereby it is only via a variable magnitude that the tilt angle can be inferred in a much less reliable way (Fig. 4). This property can be advantageously exploited in the case of particles dispersed in a matrix, as exemplified below.

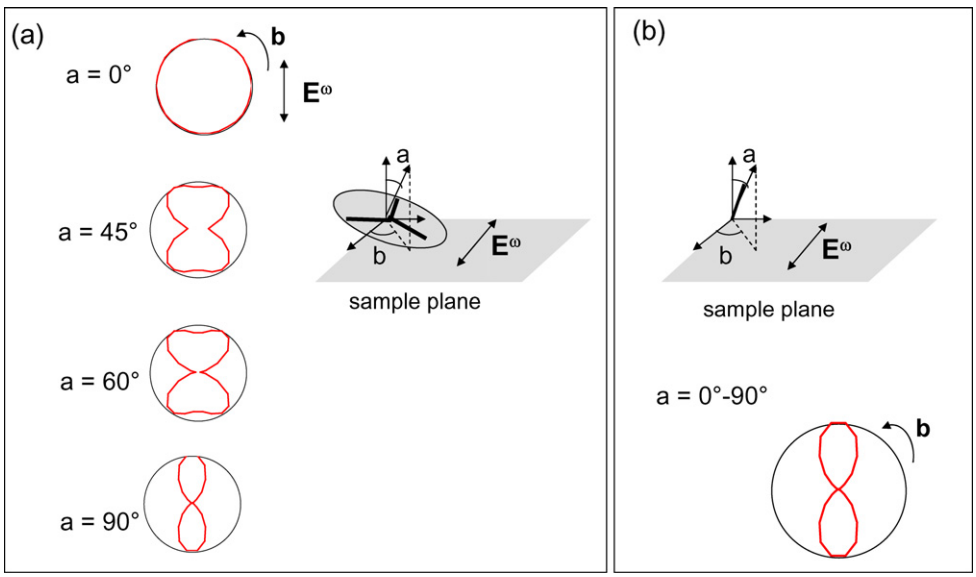

Fig. 4. Different SHG responses expected when rotating crystals of different symmetries in the sample plane: (a) planar octupolar D_{3h} symmetry (displaying strong pattern shape dependence); (b) one-dimensional symmetry (displaying only a rescaling factor).

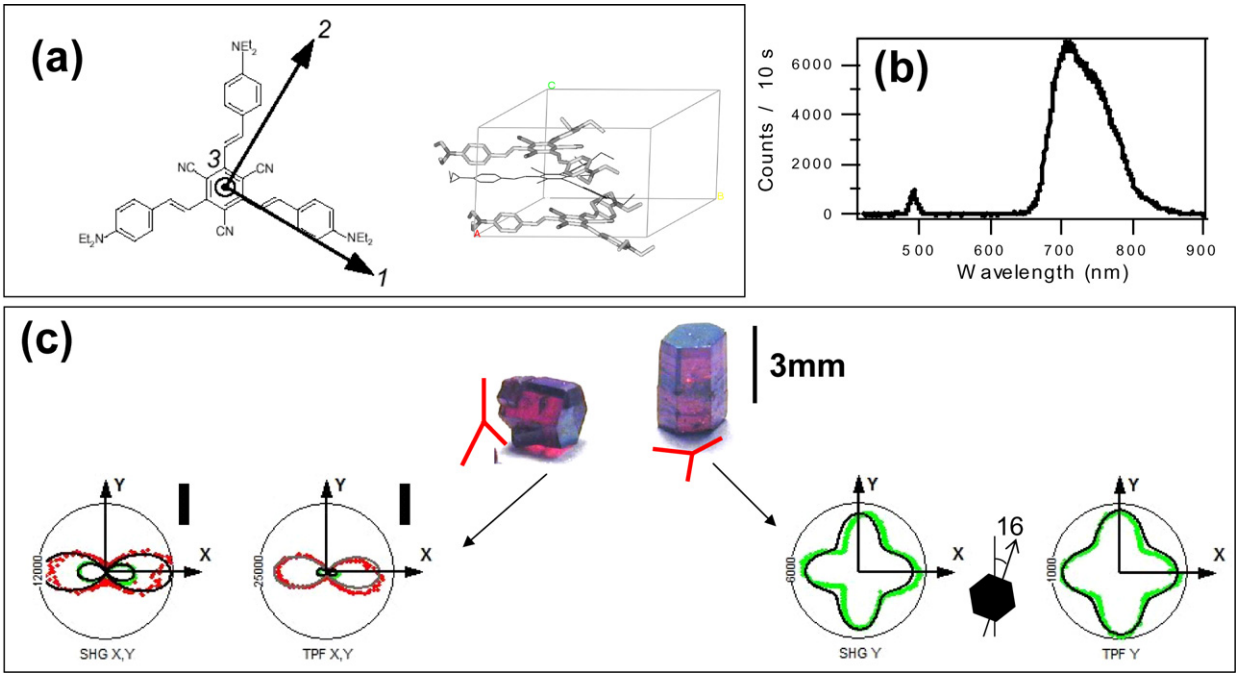

Fig. 5. Nonlinear microscopy on TTB octupolar crystals, of cylindrical shape with hexagonal sections and millimetric size: (a) three-dimensional arrangement of TTB molecules packed along the *c* axis with a slight offset; (b) measured emission spectrum exhibiting SHG and TPF; (c) nonlinear polarimetry on SHG and TPF responses for different orientations. From Ref. [21].

At the macroscopic scale, TTB octupolar crystals have been investigated in order to demonstrate the pure octupolar nature of the nonlinear response. Depending on the crystal orientation and accounting for experimental parameters such as objective numerical aperture and dichroic reflexion coefficients and phase shifts, the SHG and TPF polarization could be simultaneously adjusted. In the case where the octupoles lie within the sample plane, the polarization response is isotropic (deformations are due to microscope corrections), whereas a tilt angle tends to make the polar plots resemble a one-dimensional response, since a side-way projection of a planar octupole is similar to a dipolar one (Fig. 5).

4. Analyzing nonlinear properties from multipolar micro- and nanocrystals

Investigating micro- and nanocrystals using polarized nonlinear microscopy offers the unique advantage of allowing us to retrieve the properties of a single entity down to a size which is not otherwise amenable to usual macroscopic techniques. This technique, therefore, substitutes the traditional powder measurements to a single particle investigation, moreover benefiting from a statistical approach to crystalline quality studies. In addition, estimation of nonlinear efficiency from such objects is made possible by direct comparison with reference crystals, along the same lines as for the macroscopic approach. In this section, we describe recent attempts in obtaining nonlinear crystals of submicrometric sizes of different geometries, following different preparation schemes.

4.1. Sensitivity to disorder, symmetry and orientation

In this part we illustrate the advantage of de-coupling two analysis directions (denoted X and Y) in the polarization response measurement of SHG and TPF signals. Fig. 6 shows the dependence of the SHG polarization patterns depending on the orientational distribution nature of the nonlinear dipoles arranged according to a given symmetry pattern. It clearly shows a continuous variation of the SHG polarization responses in-between the two extreme cases of complete disorder and perfect one-dimensional order. Such dependencies are a direct signature of the crystalline degree of a molecular assembly, making SHG a unique tool to detect the degree of order in molecular structures.

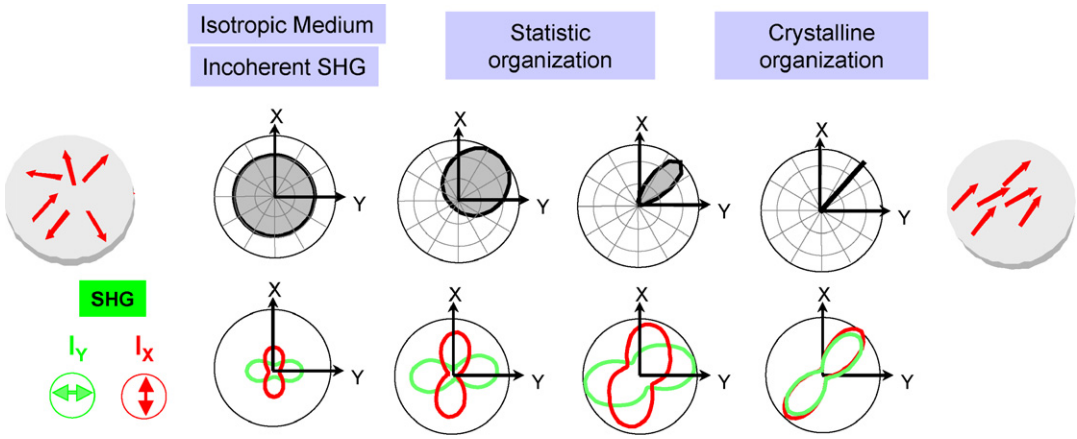

Fig. 6. SHG polarimetry analysis as a sensitive probe for crystalline disorder.

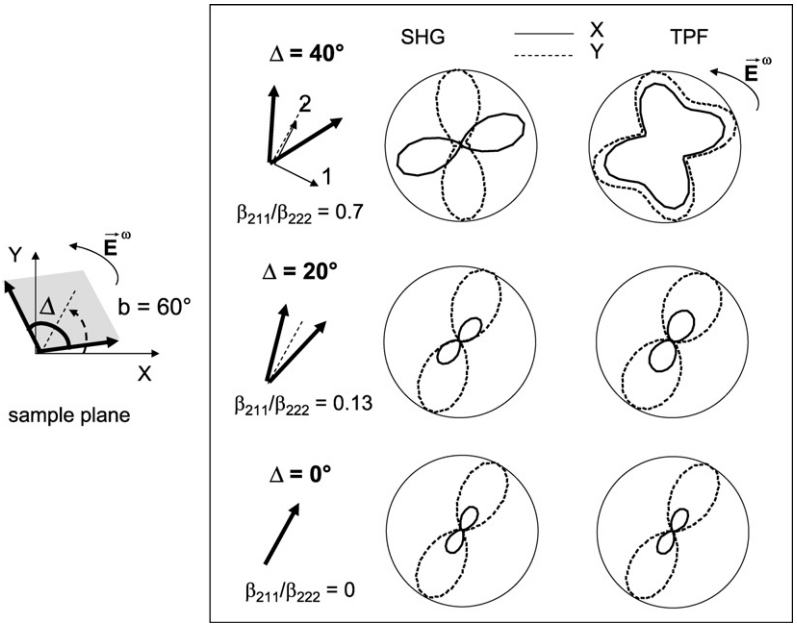

Fig. 7. Sensitivity of SHG and TPF polarization responses to crystalline nature: case of a multipolar C_{2v} unit-cell with a variable microscopic anisotropy (provided by a variation of the angle Δ between the two 1D molecules constituting the unit cell).

Fig. 7 illustrates the dependence of SHG and TPF polarization responses depending on the microscopic nonlinear anisotropy of a crystalline structure. In the C_{2v} symmetry case, which has been chosen here for simplicity, this anisotropy can be quantified by the ratio β_{211}/β_{222} with the notations of Fig. 7, which can be varied by the control of the angle Δ between the two dipoles making-up for the structure (the individual dipoles are assumed to be 1D oscillators). The symmetry thus varies between a pure one-dimensional structure ($\Delta = 0°$) to a centrosymmetric one ($\Delta = 180°$). Fig. 7 shows the strong dependence on the crystalline symmetry, as evidenced for SHG as well as TPF polar plots.

4.2. Octupolar crystalline micro-particles

Octupolar micro-crystals have been obtained from the dilution of a TTB molecular powder in water. This simple process allows us to obtain objects down to sub-micrometric size, yet not fully controlled in size and in some cases subject to aggregation of particles. The mean particle diameter obtained in such conditions is of the order of 600 nm,

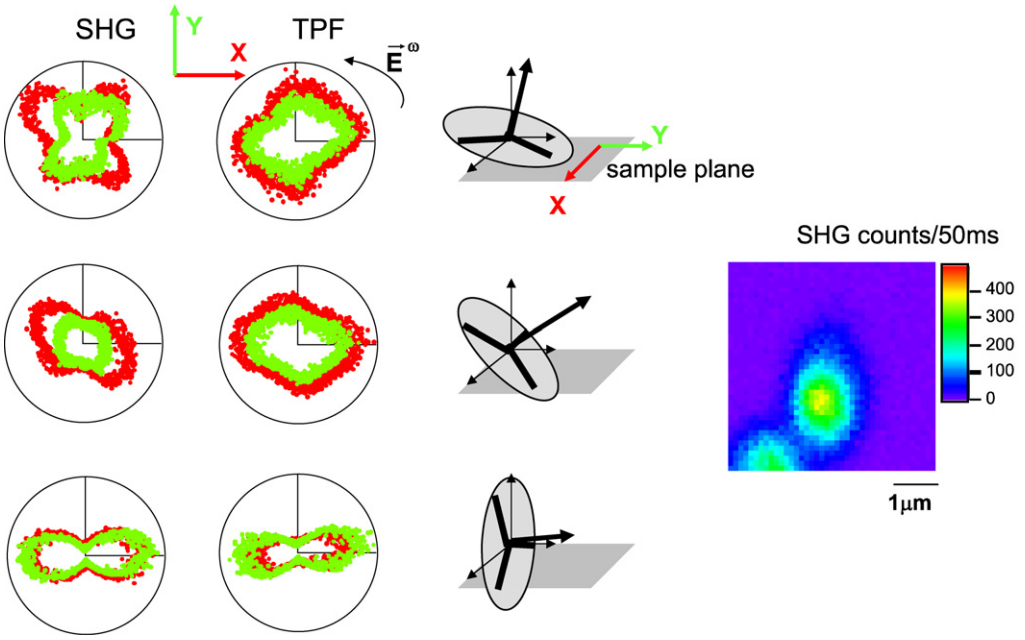

Fig. 8. TTB octupolar micro-particles resolved by SHG and TPF microscopy. The SHG scan exhibits SHG-active particles of micrometric size (TPF scans exhibit similar features). The SHG and TPF polarization analysis resolves the orientation angle of octupolar particles: close to in-plane, tilted, and orthogonal to the sample plane.

as measured from fluorescence or SHG scans over a few tens of particles. A nonlinear polarimetry analysis has been carried out on such objects, so as to benefit from the unique features of SHG and TPF in octupolar geometries, as discussed above. From the polarization responses (Fig. 8) of many sub-micrometric crystals, specific conclusions can be readily drawn: (i) the micro-crystals are still monocrystalline, as exemplified by the identical shapes obtained in the TPF polar plots for X and Y analyses directions; (ii) the polarization response resemble the macroscopic crystal ones, and can be used to evaluate the tilt angle of the particles in the polymer matrix. This, furthermore, tends to confirm the octupolar nature of such particles.

More refined nanoparticle fabrication techniques are currently under investigation with the restriction to preserve the octupolar symmetry. Such particles are interesting for orientation angle tracking, since the polarization response is a direct signature of tilt angles. Conversely, nanoparticles made-up of 3D octupoles such as abiding to tetraedral symmetry (as opposed to planar octupoles as described above) should exhibit much less angular dependence and therefore be faithful labels with limited orientational extinction as the nanoparticle is rotated around.

4.3. 3D orientation determination in multipolar nanocrystals

In addition to the specificity of octupolar symmetry, where the direct observation of polarization responses reveals 3D orientation information, it can be shown that nonlinear SHG and TPF polarization analysis provide tilt angle information in the more general case of multipolar symmetry. Such a property is verified, except for a few specific orientations where there is still an ambiguity for polarization responses which keep the same shape whatever the tilt angle of the unit cell. This can be explained by the fact that a multipolar symmetry orientation is in general characterized by three angles (θ, ϕ, ψ) defining the Euler set of angular parameters. The projection of such a symmetry in the sample plane, defined by the θ tilt angle, will therefore lead to different shapes depending on (ϕ, ψ). Such a property clearly benefits from the complementary nature of SHG and TPF relative to the order parameter of the symmetry being investigated. This is furthermore exemplified in the following example.

The α-((4′-methoxyphenyl)methylene)-4-nitro-benzene-acetonitrile) molecule (CMONS) exhibits both efficient luminescence and quadratic nonlinearity under two-photon excitation. Among the three bulk crystalline phases which co-exist in CMONS bulk crystals, the most stable one is non-centrosymmetric exhibiting close to C_{2v} symmetry [8,14,41]. The preparation of the organic nanocrystals in sol–gel glasses relies on the control of the nucleation and

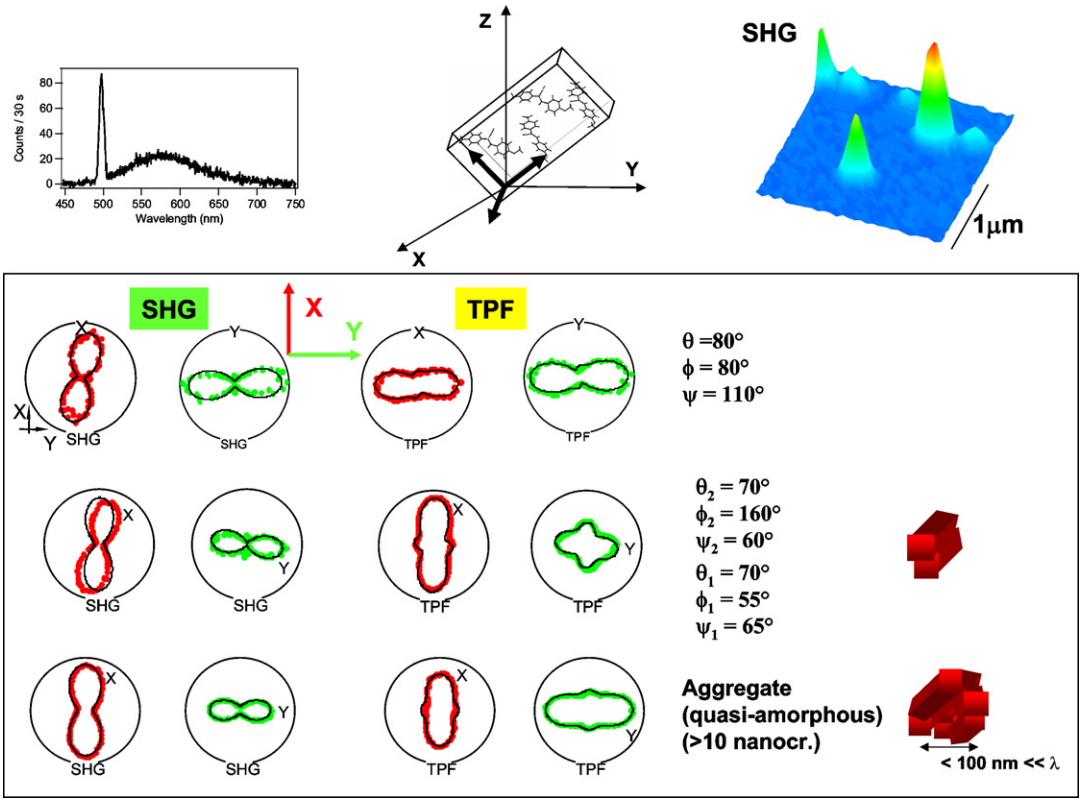

Fig. 9. Orientation determination, and crystalline diagnosis on nonlinear nanocrystals. CMONS nanocrystals grown in 1:1 tetramethoxysilane (TMOS) : methyltrimethoxysilane (MTMOS) matrices. The particles are obtained using a CMONS:alkoxydes molar fraction of 4×10^{-3}. From Ref. [14].

growth kinetics of the dye confined in the pores of the gel [8]. The particles mean size, which depends on the preparation parameters such as temperature and matrix porosity, ranges from 20 to 100 nm.

In the few examples given in Fig. 9, it can be noted that the crystalline quality is readily observed from the identification of the TPF polar plots, as discussed above. Among the pure crystalline nanostructures, the 3D orientation angles could be determined without ambiguity, adjusting simultaneously the SHG and TPF X and Y responses as a function of the three (θ, ϕ, ψ) angular parameters [14]. Further numerical studies have shown that a direct measurement of the SHG and TPF anisotropy (defined as $(X + Y)/(X - Y)$ measured for a fixed incident polarization), is sufficient to reduce the ambiguity on the orientation angles to 1 or 2 possibilities [29]. Such ambiguity can be resolved by observing the shape of the polarization responses.

5. Dipolar radiation from nonlinear nanosources

As already mentioned in Section 3.2, dipolar micro- and nanocrystals can be obtained from PHTP crystals doped with nonlinear molecules. Grinding and sonication of a mixture of DANA-PHTP millimetric size crystals in a polyvinylalcohol (PVA, 1% in H_2O) solution allows us to obtain a priori non-centrosymmetric structures of reduced size (the DANA-PHTP structure is depicted in Fig. 3). The obtained suspension of ground particles was then further diluted to reduce their concentration to approximately 1 particle/μm^3 and filtered through a 200 nm Nylon filter. The final polymer solution was then deposited by spin-coating or evaporated on a microscope coverslip. The sizes of the probed particles can be directly monitored by TPF or SHG optical microscopy.

From deconvolution in SHG images accounting for the optical excitation volume in the microscope, the sizes of the obtained particles can be determined down to a lower limit of about 80 nm, reaching up to 1 μm. The polarization SHG responses of the particles showed generally two-lobe patterns characteristic of a 1D monocrystalline structures as expected. The largest micrometric objects are, however, seen to be mostly aggregates of smaller particles, with close

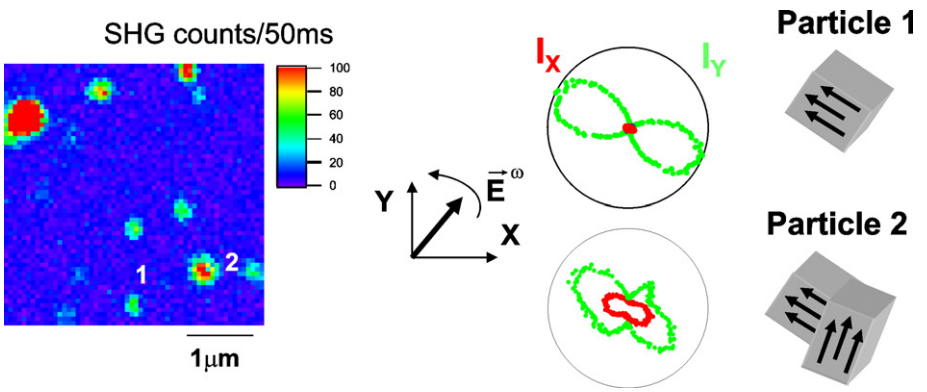

Fig. 10. PHTP-DANA micro- and nanoparticles revealed by SHG imaging. Polarimetry analysis reveals monocrystalline phase in nanosizes particles, and a major part of more complex polarization patterns in the case of micrometric sizes particles. This is characteristic of aggregation.

to isotropic polarization responses (Fig. 10). The nonlinear SHG efficiencies of sub-micrometric objects was evaluated accounting for their in-plane polarization response, and the lower limit of nonlinear coefficients was estimated to be $d_{33}(0) = 30\ \mathrm{pm\,V^{-1}}$ in 100 nm size particles [42]. This efficiency, representative of efficient SHG nanosources, is consistent with monocrystalline nano-objects following an oriented gas model approach.

The nonlinear polarimetry analysis of 1D PHTP-based structures does not allow for a direct measurement of 3D orientation, as mentioned above. The access to off-plane tilt angle, which is determinant to evaluate the exact efficiency of such nanoparticles, is however possible using additional techniques that can be implemented together with polarimetry analyses. Such techniques have been mainly developed in fluorescence microscopy dedicated to the orientation measurement of single molecule dipolar emitters. They involve complex axial excitation schemes, variable incident angle measurements or defocussing imaging methods [43,44]. An imaging measurement of dipole 3D orientation has been adapted from the defocussing imaging technique, which rely on the projection in a defocussed imaged plane of the radiation from an emitting dipole [45]. A tilted dipole will induce radiation patterns which are sensitive to its orientation, as expected from the geometrical nature of the scattering process. Such method can be transferred to the nonlinear coherent emission of SHG induced dipoles, where the direction of the nonlinear dipole is in the present case coherently related to the incident polarization [42]. In the 1D nonlinear dipole case such as in PHTP-based compounds, the emission reduces to a single direction, since only one nonlinear coefficient is dominant. Therefore the radiation pattern shapes provides directly information on the tilt angle of such dipoles (Fig. 11).

6. Conclusions

Molecular crystals have played a seminal role in the early days of molecular nonlinear optics by virtue of their well ordered lattice allowing a quasi one-to-one connection between molecular to macroscopic properties. Indeed, the oriented gas model has served generations of researchers in permitting them to infer microscopic tensor components from bulk nonlinear optical susceptibilities as from usual free space second-harmonic and related frequency mixing configurations. Whereas this interplay between solution, powder solid state and experiments on the one hand, and modelling on the other hand had set a deep imprint over nearly two decades of molecular nonlinear optics studies, well into the 1980s, the advent of polymer functional structures, more prone to technology and the subsequent delivery of devices had diverted the mainstream interest of the community away from single crystals, except from some specific ongoing fundamental studies.

The advent of nanotechnologies and nanophotonics has revitalized the domain of single crystalline molecular nonlinear optics, thanks to the ability to grow tailored nanocrystals in a controlled way and moreover to the accompanying development of microscopic instrumentation capable to downscale nonlinear investigations, quantitatively so, down to a scale that was previously vaguely referred to as a powder ‘grain’, liable at best to a semi-quantitative powder test crude scan investigation [46]. Far from being a ‘tour de force’ per se, the growth and characterization of nanocrystals, be they purely organic, or of the guest–host or hybrid type, opens-up new possibilities in terms of materials and even devices that could take advantage of both the versatility of polymer templates and of the unique properties of single crystalline nanoparticles embedded therein.

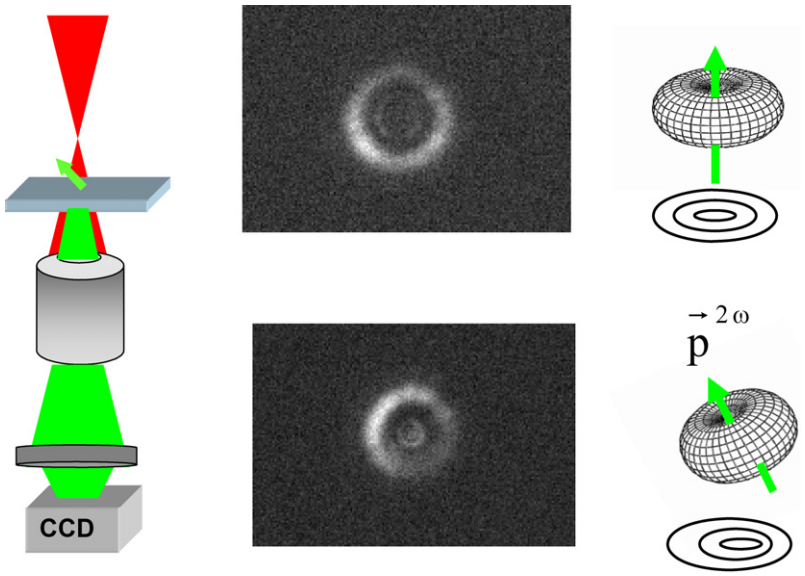

Fig. 11. Dipole radiation pattern imaging technique applied to 1D PHTP-DANA nanoparticles. 3D orientation determination. From Ref. [42].

We have shown in this review that nonlinear polarimetry of nanocrystals or of inhomogeneous materials, has become a realistic possibility, as demonstrated herein in various cases spanning different states of molecular matter and symmetry constraints. The increased availability of powerful advanced multi-photon microscopes endowed with sensitive polarimetric and phase control as well as detection schemes entail the possibility to map at submicron scale the distribution of order parameters in arbitrary media, with biological media and in particular cells as a major target. Such instrumental possibilities, in conjunction with the development of nanotechnologies as well as biotechnologies, open-up new horizons in nonlinear photonics and nonlinear imaging at ultimate scales that can truly be considered as a revival of nonlinear optics onto new frontiers of material and life sciences.

Acknowledgements

We would like to acknowledge Véronique Le Floc'h, Katarzyna Komorowska, Peter Frederiksen, for the work on nonlinear microscopy, Estelle Botzung-Appert and Alain Ibanez (Université Grenoble, France), Bong Rae Cho (Seoul University, Korea), Lars Poulsen, Mickael Jazdzyk, Hans-Joachim Egelhaaf, Johannes Gierschner, Michael Hanack (University of Tübingen), for the collaborations on nonlinear crystalline structure. This work was partially supported by the Directorate of General Research of the EC, RTN NANOCHANNEL (Grant No. HPRN-CT-2002-00323) and by Ministère de la Recherche, France.

References

[1] T. Seko, K. Ogura, Y. Kawakami, H. Sugino, H. Toyotama, J. Tanaka, Excimer emission of anthracene, perylene, coronene and pyrene microcrystals dispersed in water, Chem. Phys. Lett. 291 (1998) 438–444.
[2] Y. Wang, K. Deng, L. Gui, Y. Tang, J. Zhou, L. Cai, J. Qiu, D. Ren, Y. Wang, J. Colloid. Interface Sci. 213 (1999) 270.
[3] K. Baba, H. Kasai, S. Okada, H. Oikawa, H. Nakanishi, Fabrication of organic nanocrystals using microwave irradiation and their optical properties, Opt. Mater. 21 (2002) 591–594.
[4] Y. Tamaki, T. Asahi, H. Masuhara, Nanoparticle formation of vanadyl phtalocyanine by laser ablation of its crystalline powder in a poor solvent, J. Phys. Chem. A 106 (2002) 2135–2139.
[5] A. Ibanez, S. Maximov, A. Guiu, C. Chaillout, P.L. Baldeck, Controlled nanocrystallization of organic molecules in sol–gel glasses, Adv. Mater. 10 (1998) 1540.
[6] P.G. Lacroix, R. Clément, K. Nakatani, J. Zyss, I. Ledoux, Science 263 (1994) 658.
[7] H.B. Fu, J.N. Yao, Size effects of the optical properties of organic nanoparticles, J. Am. Chem. Soc. 123 (2001) 1434–1439.
[8] E. Botzung-Appert, V. Monnier, T. Ha Duong, R. Pansu, A. Ibanez, Polyaromatic luminescent nanocrystals for chemical and biological sensors, Chem. Mater. 16 (2004) 1609–1611;
N. Sanz, P.L. Baldeck, J.F. Nicoud, Y. LeFur, A. Ibanez, Solid State Sci. 3 (2001) 867–875.

[9] T. Yi, R. Clément, C. Haut, L. Catala, T. Gacoin, N. Tancrez, I. Ledoux, J. Zyss, J-aggregated dye–MnPS3 hybrid nano-particles with giant quadratic optical non-linearity, Adv. Mater. 17 (3) (2005) 335.
[10] G. Revillod, I. Russier-Antoine, E. Benichou, C. Jonin, P.-F. Brevet, Investigating the interaction of crystal violet probe molecules on sodium dodecyl sulfate micelles with hyper-Rayleigh scattering, J. Phys. Chem. B 109 (2005) 5383.
[11] M. Flörsheimer, M. Bösch, Ch. Brillert, M. Wierschem, H. Fuchs, Thin Solid Films 327 (1998) 241.
[12] C. Anceau, S. Brasselet, J. Zyss, Local orientational distribution of molecular monolayers probed by nonlinear microscopy, Chem. Phys. Lett. 411 (1–3) (2005) 98–102.
[13] C. Anceau, S. Brasselet, P. Gadenne, J. Zyss, Local second harmonic generation enhancement on gold nanostructures probed by 2-photon microscopy, Opt. Lett. 83 (2003) 2681–2692.
[14] S. Brasselet, V. Le Floc'h, F. Treussart, J.F. Roch, J. Zyss, E. Botzung-Appert, A. Ibanez, In situ diagnostics of the crystalline nature of single organic nanocrystals by nonlinear microscopy, Phys. Rev. Lett. 92 (20) (2004) 207401.
[15] N. Tancrez, S. Brasselet, I. Ledoux, J. Zyss, Nonlinear optical properties of J-aggregated dye–MnPS3 hybrid nano-particles, submitted for publication.
[16] L. Moreaux, O. Sandre, M. Blanchard-Desce, J. Mertz, Membrane imaging by simultaneous second-harmonic generation and two-photon microscopy, Opt. Lett. 25 (2000) 320–322.
[17] V. Le Floc'h, S. Brasselet, J.F. Roch, J. Zyss, Monitoring of orientation in molecular ensembles by polarization sensitive nonlinear microscopy, J. Phys. Chem. B 107 (2003) 12403–12410.
[18] J. Zyss, Nonlin. Opt. 1 (1991) 3;
J. Zyss, Molecular engineering implications of rotational invariance in quadratic nonlinear optics: from dipolar to octupolar molecules and materials, J. Chem. Phys. 98 (1993) 6583.
[19] S. Brasselet, J. Zyss, Multipolar molecules and multipolar fields: probing and controlling the tensorial nature of nonlinear molecular media, J. Opt. Soc. Am. B 15 (1) (1998) 257.
[20] J. Zyss, S. Brasselet, V. Thalladi, G. Desiraju, Octupolar versus dipolar crystalline structures in nonlinear optics. A dual crystal and propagative engineering approach, J. Chem. Phys. 109 (2) (1998) 658.
[21] V. Le Floc'h, S. Brasselet, J. Zyss, B.R. Cho, S.H. Lee, S.J. Jeon, M. Cho, K.S. Min, M.P. Suh, High efficiency and quadratic nonlinear optical properties of a fully optimized 2-D octupolar crystal by nonlinear microscopy, Adv. Mater. 17 (2) (2005) 196–200.
[22] B. Boulanger, G. Marnier, Opt. Commun. 79 (1990) 102.
[23] S. Bidault, S. Brasselet, J. Zyss, Coherent control of the optical nonlinear and luminescence anisotropies of molecular thin films by multiphoton excitations, Opt. Lett. 29 (11) (2004) 1242–1244.
[24] A.D. Buckingham, R.L. Disch, Proc. Royal Soc. A 273 (1963) 275.
[25] E.P. Wigner, Group Theory, Academic Press, New York, 1959.
[26] D.S. Chemla, J.L. Oudar, J. Jerphagnon, Origin of the second-order optical susceptibilities of crystalline substituted benzene, Phys. Rev. B 12 (10) (1975) 4534–4546.
[27] J. Zyss, J.L. Oudar, Relationship between microscopic and macroscopic lowest order optical nonlinearities of molecular crystals with one- and two-dimensional units, Phys. Rev. A 26 (1982) 2028–2048.
[28] L. Moreaux, O. Sandre, M. Blanchard-Desce, J. Mertz, Simultaneous second-harmonic generation and two-photon excited fluorescence microscopy, Nonlin. Opt. 25 (2000) 183–188.
[29] V. Le Floc'h, PhD thesis, ENS Cachan, France, 2003.
[30] H. Vanherzeele, J.D. Bierlein, Magnitude of the nonlinear-optical coefficients of $KTiOPO_4$, Opt. Lett. 17 (1992) 982.
[31] H. Nakanishi, H. Matsuda, S. Okada, M. Kato, in: Proceedings of the MRS International Meeting on Advanced Materials, vol. 1, 1989, 143.
[32] H. Oikawa, S. Fujita, H. Kasai, S. Okada, S.K. Tripathy, H. Nakanishi, Colloids and Surfaces A: Physicochem. Eng. Aspects 169 (2000) 251.
[33] I. Weissbuch, M. Lahav, L. Leiserowitz, G.R. Meredith, H. Vanherzeele, Chem. Mater. 1 (1989) 114.
[34] J. Hulliger, P. Rogin, A. Quintel, P. Rechsteiner, O. Konig, M. Wuebbenhorst, Adv. Mater. 9 (1997) 677.
[35] A. Quintel, J. Hulliger, M. Wuebbenhorst, J. Phys. Chem. B 102 (1998) 4277.
[36] P. Rechsteiner, J. Hulliger, M. Flosheimer, Chem. Mater. 11 (2000) 3296.
[37] K. Komorowska, S. Brasselet, J. Zyss, L. Pourlsen, M. Jazdzyk, H.J. Egelhaaf, J. Gierschner, M. Hanack, Nanometric scale investigation of the nonlinear efficiency of perhydrotriphynylene inclusion compounds, Chem. Phys. 318 (1–2) (2005) 12–20.
[38] V.R. Thalladi, S. Brasselet, H.-C. Weiss, D. Bläser, A.K. Katz, H.L. Carell, R. Boese, J. Zyss, A. Nangia, G.R. Desiraju, J. Am. Chem. Soc. 120 (1998) 2563.
[39] B.R. Cho, S.B. Park, S.J. Lee, K.H. Son, S.H. Lee, M.-J. Lee, J. Yoo, Y.K. Lee, G.J. Lee, T.I. Kang, M. Cho, S.-J. Jeon, J. Am. Chem. Soc. 123 (2001) 6421.
[40] J. Zyss, I. Ledoux-Rak, H.C. Weiss, D. Bläser, R. Boese, P.K. Thallapally, V.R. Thalladi, G.R. Desiraju, Coupling octupoles in crystals: the case of the 1,3,5-trinitrobenzene-triphenylene1:1 molecular co-crystal, Chem. Mater. 15 (2003) 3063–3073.
[41] R.M. Vrcelj, E.E.A. Shepderd, C.Y. Yoon, J. Sherwood, A.R. Kennedy, Preparation evaluation of the conformational polymorphs of α-[(4-Methoxyphenyl)methylene]-4-nitrobenzeneacetonitrile, Crystal Growth Design 2 (2002) 609.
[42] K. Komorowska, L. Pourlsen, M. Jazdzyk, S. Brasselet, SHG microscopy investigation of PHTP inclusion compounds based nanoparticles, in preparation.
[43] B. Sick, B. Hecht, L. Novotny, Orientational imaging of single molecules by annular illumination, Phys. Rev. Lett. 85 (2000) 4482–4485.
[44] M. Vacha, M. Kotaki, Three-dimensional orientation of single molecules observed by far- and near-field fluorescence microscopy, J. Chem. Phys. 118 (12) (2003) 5279–5282.
[45] M. Böhmer, J. Enderlein, Orientation imaging of single molecules by wide-field epifluorescence microscopy, J. Opt. Soc. Am. B 20 (3) (2003) 554–559.
[46] S.K. Kurtz, T.T. Perry, J. Appl. Phys. 39 (1968) 3798–3813.